epoxide (Table III) to 31% under anaerobic conditions is probably due to formation of epoxide by reaction of alkene with a decomposition product of **2**. The probability of this being so stems from the lack of effect of olefin on the rate constant for disappearance of **2** from solution. Also, the direct transfer of an oxygen from **2** to olefin to form epoxide should produce the flavin-derived alcohol 4a-FlEtOH in yield comparable to that of epoxide (eq 12). This was not found to be the case (Table III). Though 4a-FlEtOH decomposes in the chloroform solvent employed, the rate constant for this reaction is sufficiently slow to allow a reasonable determination of the percent yield of 4a-FlEtOH. The principal (90%) decomposition product of **2**, in these experiments, was the 10a-spirohydantoin C. The formation of 10a-spirohydantoins as decomposition products of flavin 4a-hydroperoxides have been noted previously,[36,32b] and their structures have been established by X-ray crystallography.[32b] Spirohydantoin C does not form from 4a-FlEtOH in $CHCl_3$ so that the high yield of C determined in the epoxidation reactions assures the low yield of 4a-FlEtOH and proves that the epoxide does not arise by direct reaction of **2** and olefin (eq 12). Mager reports that a suspension of **2** in H_2O yields C and molecular oxygen (stoichiometry not reported) and proposed the reaction to occur through the carbonyl oxide I (eq 16).[36] The driving force for the formation of I from **2** is not apparent, but if the proposal of the formation of I should be correct, it would supply an epoxidizing species. As previously noted, the hydroperoxide **2** does decompose in $CHCl_3$ by a kinetically apparent two-step mechanism as required by Mager's proposed reaction. The rate constants associated with neither step is, however, changed by the presence of alkene. This feature does not support I as an epoxidation agent in the decomposition of **2**. Perhaps epoxidation occurs by reaction of olefin with oxygen liberated on decomposition of **2** (eq 16). One might note that the yield of epoxide is doubled when **2** and alkene are combined in $CHCl_3$ in the presence of air (Table III).

4a-Hydroperoxylflavins Are the Only Known Hydroperoxides Which Exhibit a Chemiluminescent (CL) Oxidation of Aldehydes.[37]

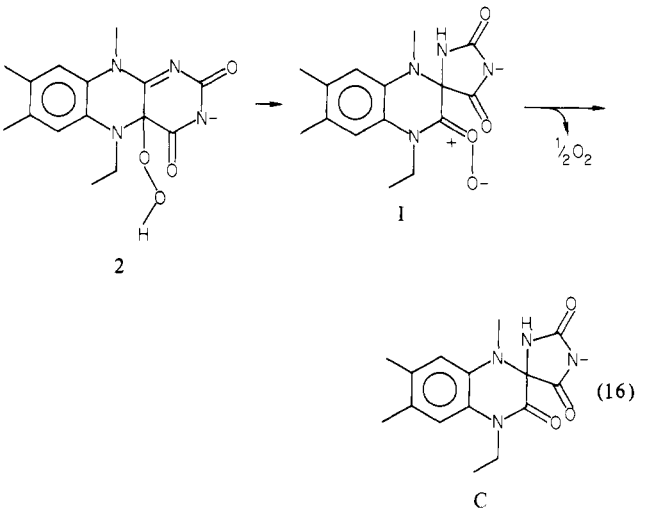

Thus, *no light* emission is noted when **4**, **5**, and **6** are allowed to react with *p*-tolualdehyde. The reaction of **2** with *p*-tolualdehyde in absolute *t*-BuOH provides CL with $\Phi \cong 5 \times 10^{-4}$.[38]

Acknowledgment. This work was supported by grants from the National Institutes of Health and the National Science Foundation.

Registry No. **1**, 937-14-4; **2**, 59587-26-7; **3**, 79075-90-4; **4**, 5233-67-0; **5**, 57272-44-3; **6**, 30152-69-3; **7**, 7722-84-1; **8**, 75-91-2; iodide, 20461-54-5; thioxane, 15980-15-1; *N,N*-dimethylbenzylamine, 103-83-3; 2,3-dimethyl-2-butene, 563-79-1; *p*-tolualdehyde, 104-87-0.

(36) Mager, H. I. X. *Tetrahedron Lett.* **1979**, 3549.

(37) Kemal, C.; Bruice, T. C. *J. Am. Chem. Soc.* **1977**, *99*, 7064.
(38) Shepherd, P. T.; Bruice, T. C. *J. Am. Chem. Soc.* **1980**, *102*, 7774.
(39) Ball, S.; Bruice, T. C. *J. Am. Chem. Soc.* **1981**, *103*, 5494.
(40) Kemal, C.; Chan, T. W.; Bruice, T. C. *Proc. Natl. Acad. Sci. U.S.A.* **1977**, *74*, 405.

Conformational Energies of Fenfluramine: Graphical Representation of Energy as a Function of Four Conformational Variables

Mary Weir Creese and Gary L. Grunewald*

Contribution from the Department of Medicinal Chemistry, University of Kansas, Lawrence, Kansas 66045. *Received May 20, 1982*

Abstract: We have investigated the low-energy conformations of the protonated form of fenfluramine [*m*-(trifluoromethyl)-*N*-ethylamphetamine] using CAMSEQ.[1-3] All four of the torsion angles in the (*N*-ethylamino)propyl side chain have been examined. The results are presented as (a) τ_1–τ_2 energy maps for both solution and vacuum, the in vacuo map shaded to show areas corresponding to particular τ_3–τ_4 conformations, and (b) "three-dimensional" representations illustrating variation in energy as a function of three variables, the fourth variables taken as a parameter. The in vacuo minimum-energy conformation found for fenfluramine has $\tau_1 = 240°$, $\tau_2 = 70°$, $\tau_3 = 300°$, and $\tau_4 = 300°$, and the barrier between the minimum-energy conformation and the extended form ($\tau_2 = 180°$) is ≈6.5 kcal/mol. Conformation changes in τ_1–τ_2 are shown to be coupled with changes in τ_3–τ_4. In aqueous solution the extended form of fenfluramine is found to be the more stable by ≈27 kcal/mol.

Fenfluramine is of interest pharmacologically because it functions as an appetite depressant in animals without simultaneously acting as a psychomotor stimulant.[4-11] Thus, it has potential use as an anorectic agent free from "drug abruse" dif-

(1) Weintraub, H. J. R. Ph.D. Dissertation, Case Western Reserve University, Cleveland, OH, 1975.

(2) Weintraub, H. J. R.; Hopfinger, A. J. *Int. J. Quantum Chem., Quantum Biol. Symp.* **1975**, *No. 2*, 203–208.

0002-7863/83/1505-2463$01.50/0

ficulties.[12-14] Since the efficacy of a drug molecule is in part dependent on successful interaction with the receptor site, and since this in turn is likely to be in part dependent on conformation, an acquaintance with the basic conformational energetics of the system is of interest. Most of the results presented deal with conformational energies in vacuo, and it has been argued that such data may not shed any light on what happens in aqueous media (e.g., in vivo). Indeed, the results we show for solution calculations indicate that energies and conformational preferences of fenfluramine are quite different in this medium; here the extended form (τ_2 = 180°) is the more stable by 27 kcal/mol, a figure which overshadows differences in conformational energies in vacuum by a factor of 4.5. However, if we consider that, having entered the receptor site, the drug molecule may not be solvated, and also that the details of the entry process, e.g., the redistribution and eventual loss of solvent molecules, are less than clearly understood at present, the procedure of determining conformational energetics of a molecule in the simplest environment, namely, in vacuum, remains a reasonable starting point in the investigation of the pharmacological mode of action of conformationally labile molecules. That is, the conformational preferences of the molecule in vacuum constitute basic information, to which necessary elaborations and refinements can be added.

Since the molecule is quite big (32 atoms) we have not at this stage used calculational methods allowing simultaneous relaxation of bond lengths and angles with changes in torsion angles. Torsion angles being the most important factor influencing conformational energy differences, the investigation is restricted to these.

To get useful conformational energy information about fenfluramine, it is necessary to consider systematic simultaneous rotations of all four torsion angles in the (*N*-ethylamino)propyl side chain. The number of energy value calculations (data points) this would involve (12^4 = 20 736 for a four-dimensional map with the rotations taken at 30° intervals) rules out calculational methods in which each energy value requires a separate input by hand. The CAMSEQ software system allows the user to make, in a single run, calculations at all points (τ_1, τ_2, ..., τ_n), the range and increment for each variable being specified separately.

Experimental Procedures

Starting data consisted of the fractional coordinates found in the X-ray examination of fenfluramine.[15]

Previous conformational energy investigations[16-21] of phenethylamine-type systems have involved the preparation of τ_1–τ_2 energy maps. Since we must deal with four variables here, the final map must necessarily be produced stepwise[22] and the process is necessarily more complex than the investigation of the energy surface of a two-torsion-angle molecule such as amphetamine.

The first step was the preparation of a set of twelve τ_1–τ_2 energy maps (with 30° increments from 0° to 330° in τ_1 and τ_2) for values of τ_3 ranging from 0° to 360°. τ_4 was fixed at 180°, its value in the crystal. This provided a crude picture of energy variation as a function of τ_1, τ_2, and τ_3 (for τ_4 = 180°), and it indicated approximate periodicity as a function of τ_1 with a period of 180°. This meant that the calculation could be cut in half, and only one half-plane need be considered: 180° ≤ τ_1 ≤ 360°. The preliminary picture also delineated the high energy areas of no interest which could be neglected. The energy surfaces were generally similar to those observed for amphetamine,[16-20] with a low-energy region for the fully extended trans-anti-periplanar form, at τ_2 = 180°, and two low-energy regions for the folded gauche conformations at τ_2 = 60° and 120°. These three low-energy regions were separated by barriers whose height appeared to be <10 kcal/mol.

The influence of τ_4 on the energy was investigated initially by making a set of 30° increment τ_3–τ_4 maps for fixed τ_1–τ_2 values that were of interest. This accomplished two things: it allowed further lowering of the energy at points of interest in the τ_1–τ_2 grid, and it provided a crude sketch of energy variation with τ_3–τ_4. These τ_3–τ_4 maps also emphasized the fact that there were a limited number of preferred conformations for the chain that need be considered. Theoretically there are 27 possible staggered conformations for the chain if we consider the staggered combinations of τ_2, τ_3, and τ_4 and 9 if we consider only τ_3 and τ_4. τ_1–τ_2 maps at 10° increments were run for all nine of the possible staggered conformations of τ_3–τ_4. Four of these nine conformations—(τ_3, τ_4) = (300°, 300°), (300°, 180°), (60°, 180°), and (180°, 60°)—turned out to be important in the energy picture, though the theoretical values for the torsion angles are not assumed exactly (±20° spread). Again these 10° increment maps were also useful in the search for lower minimum energy values in important regions of the main τ_1–τ_2 map.

The preceding collection of calculations was sufficient to provide fairly definite data about the locations of the low-energy regions and the ridges between these regions. The bottoms and sides of the low-energy hollows were further investigated by a series of 10° searches τ_3–τ_4 and by minimizations in four variables at 10° increments over limited regions of space. The barriers between the low-energy regions were investigated in a similar manner. The 10° searches proved to be worthwhile refinements over the 30° searches and had the effect of lowering energy values by 1–2 kcal/mol.

Thus, the main τ_1–τ_2 map (Figure 1) shows energy minimizations on τ_3–τ_4. For each pair (τ_1, τ_2), only one energy value (the minimum energy) from the corresponding τ_3–τ_4 map (either 30° increment or 10° at important locations) is used. (Alternatively, as implied above, an energy in the τ_1–τ_2 map may have been arrived at by a four-variable search in 10° increments over a limited area.) The shading over the τ_1–τ_2 map is the record of the τ_3–τ_4 conformations at which the minimum in question occurred. It attempts to present more complete four-variable data on the page.

An attempt has also been made to show a "three-dimensional" map of energy variation with τ_2, τ_3, and τ_4, τ_1 being held at 280°, a value which comes close to crossing all the passes and all three low-energy regions. This picture consists of a stack of 12 τ_3–τ_4 maps at 10° increments, with τ_2 varied from 0° to 360° at 30° increments (Figure 2a). Similarly, Figure 2b shows τ_3–τ_4 maps for τ_1 = 260°, 0° ≤ τ_2 ≤ 60°. Taken together, view b and part of view a of Figure 2 give a "four-dimensional" energy contour map of the region 260° ≤ τ_1 ≤ 280°, 0° ≤ τ_2 ≤ 60°, 0° ≤ τ_3 ≤ 60°, and 0° ≤ τ_4 ≤ 360°.

Results and Discussion

A relatively efficient and inexpensive energy calculational method such as CAMSEQ makes it possible to deal with a molecule as complex as fenfluramine in fair detail, something that would have been costly, time consuming, and cumbersome by methods requiring point-by-point calculation. The final picture of energy variation as a function of τ_1, τ_2, τ_3, and τ_4, though it might still benefit from refinement in terms of effects such as bond length and bond angle relaxation, offers a useful base picture of conformational preferences.

The τ_1–τ_2 map (Figure 1) indicates that τ_1–τ_2 rotations are coupled with τ_3–τ_4 rotations. That is, changes in conformation

(3) Potenzone, R.; Cavicchi, E.; Weintraub, H. J. R.; Hopfinger, A. J. *Comput. Chem.* **1977**, *1*, 187–194.
(4) Bizzi, A.; Bonaccorsi, A.; Jespersen, S.; Jori, A.; Garattini, S. "Amphetamines and Related Compounds"; Costa, E.; Garattini, S., Eds.; Raven Press: New York, 1970; pp 577–595.
(5) Elliot, B. W. *Curr. Ther. Res. Clin. Exp.* **1970**, *12*, 502–515.
(6) Hadler, A. J. *J. Clin. Pharmacol.* **1971**, *11*, 52–55.
(7) Hooper, A. C. B. *J. Ir. Med. Assoc.* **1972**, *65*, 35–37.
(8) Le Douarec, J. C.; Neveu, C. "Amphetamines and Related Compounds"; Costa, E.; Garattini, S., Eds.; Raven Press: New York, 1970, pp 75–105.
(9) Spence, A. W.; Medvei, V. C. *Br. J. Clin. Pract.* **1966**, *20*, 643–644.
(10) Woodward, E. "Amphetamines and Related Compounds"; Costa, E.; Garattini, S., Eds.; Raven Press: New York, 1970, pp 685–691.
(11) Ziance, R. J.; Sipes, I. G.; Kinnard, W. J., Jr.; Buckley, J. P. *J. Pharmacol. Exp. Ther.* **1972**, *180*, 110–117.
(12) Tessel, R. E.; Rutledge, C. O. *J. Pharmacol. Exp. Ther.* **1972**, *197*, 252–262.
(13) Tessel, R. E.; Woods, J. H. *Psychopharmacologia* **1975**, *43*, 239–244.
(14) Woods, J. H.; Tessel, R. E. *Science (Washington, D.C.)* **1974**, *185*, 1067–1069.
(15) Grunewald, G. L.; Creese, M. W.; Extine, M. W. *Acta Crystallogr., Sect. B* **1981**, *B37*, 1790–1793.
(16) Hall, G. G.; Miller, C. J.; Schnuelle, G. W. *J. Theor. Biol.* **1975**, *53*, 475–480.
(17) Pullman, B.; Courbeils, J. L.; Courrière, Ph.; Gervois, J.-P. *J. Med. Chem.* **1972**, *15*, 17–23.
(18) Pullman, B.; Berthod, H.; Courrière, Ph. *Int. J. Quantum Chem., Quantum Biol. Symp.* **1974**, *No. 1*, 93–108.
(19) Weintraub, H. J. R.; Hopfinger, A. J. *J. Theor. Biol.* **1973**, *41*, 53–75.
(20) Grunewald, G. L., Creese, M. W.; Walters, D. E. ACS *Symp. Ser.* **1979**, *No. 112*, 439–487.
(21) Höltje, H.-D.; Vogelgesang, L. *Arch. Pharm. (Weinheim, Ger.)* **1980**, *313*, 620–635.
(22) See ref 23 for a discussion of a somewhat similar problem in six-dimensional conformational space.
(23) Hopfinger, A. J.; Battershell, R. D. *Adv. Pestic. Sci., Plenary Lect. Symp. Pap. Int. Congr. Pestic. Chem., 4th, 1978* **1979**, 196–200.

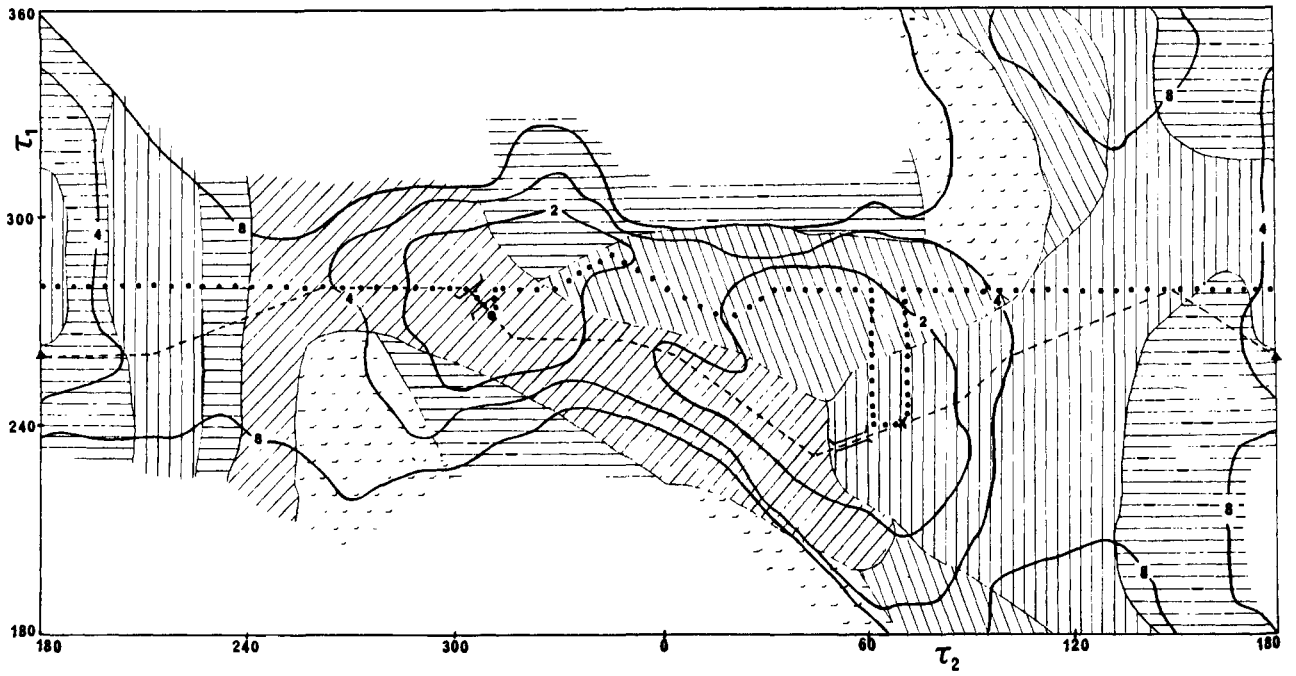

Figure 1. Fenfluramine: τ_1–τ_2 half-plane, energy minimized on τ_3–τ_4. Energies in kilocalories per mole above the global minimum, X. The symbol • at $\tau_1 = 270°$, $\tau_2 = 310°$ indicates other folded (local) minimum. Shading indicates areas of local τ_3–τ_4 conformational preference. In areas of mixed conformation (horizontal lines), all four of the prominent conformations, A, B, C, and D, are present. (Vertical lines) Conformational A, $\tau_3 = 300°$, $\tau_4 = 300°$; (left diagonal lines, \\\\) conformational B, $\tau_3 = 290°$, $\tau_4 = 140°$; (right-diagonal lines, ////) conformation C, $\tau_3 = 80°$, $\tau_4 = 200°$; (tick marks) conformation D, $\tau_3 = 180°$, $\tau_4 = 60°$; (horizontal lines) areas of several equally stable conformations. (···) and (- - -) are pathways across two representative low-energy routes. Symbols] [indicate low energy passes between major low-energy regions in τ_3–τ_4 space.

at the ring end of the (*N*-ethylamino)propyl chain are accompanied by adjustments at the *N*-ethyl end if low-energy conformations are to be maintained for the molecules as a whole. This map is quite similar to the equivalent τ_1–τ_2 map for amphetamine.[16] Thus, the change in chain length from amphetamine to fenfluramine does not greatly affect this τ_1–τ_2 energy map, provided the *N*-ethyl end of the fenfluramine chain is allowed to arrange itself in preferred conformations. Both the "minimized" fenfluramine map (Figure 1) and the amphetamine map[16] show low-energy regions at $\tau_2 \approx 60°$ and $\tau_2 \approx 300°$ and another low-energy region at $\tau_2 = 180°$, for $\tau_1 \approx 260°$. The global minimum for fenfluramine occurs in the $\tau_2 \approx 60°$ region (cf. amphetamine[16]), and the other folded conformation ($\tau_2 \approx 300°$) is represented by a low point about 1 kcal/mol higher at $\tau_2 = 310°$. The pass between the two low areas is shown as ≈2.5 kcal/mol (but see discussion of the double bridge under Graphing Procedures for Four Variables), and the barriers separating folded and extended conformations are ≈6.5 kcal/mol. ORTEP drawings (Figure 3) illustrate the preferred conformations for the folded and extended forms of fenfluramine and one of the two preferred conformations at the central ridge.

The τ_3–τ_4 maps that make up Figure 2 show the importance of the staggered τ_3–τ_4 conformations. These appear as low spots in the three-dimensional tunnels through the τ_2, τ_3, τ_4 cube (Figure 2a). The contours for a given energy level (i.e., the tunnels in the cube) are not all interconnected, and passage from one preferred conformation to another requires crossing the energy barrier between the tunnels. The latter barriers do not appear in the contours in the τ_1–τ_2 map.

Graphing Procedures for Four Variables: Figure 1, a Projection, Contrasted with Figure 2, a Diagram of Sections. In a system of this type, where there are several preferred conformations, when only some of the variables (i.e., torsion angles) are made to undergo controlled changes, the values of the remaining variables being determined by minimization, passage from one low-energy conformation (one tunnel in three space) to another appears as a conformational discontinuity. The shading in Figure 1 shows the results obtained when the system is treated in this manner, viz., when τ_1 and τ_2 are constrained to change smoothly or by small increments and τ_3 and τ_4 are determined by energy minimization. Energy variation is smooth, but the chain conformations are observed to undergo discontinuous changes. These discontinuities are introduced by the calculational method (minimization) or the equivalent graphing method (projection).[24] By contrast, in Figure 2a one variable (τ_1) is fixed and energy is plotted as a function of the other three.[25] There are no discontinuities here because τ_1 is not subjected to minimization.

The four-dimensional cube for this system ($180° \leq \tau_1 \leq 360°$, $0° \leq \tau_2, \tau_3, \tau_4 \leq 360°$) has six major wells identifiable as follows: over each of the three preferred values for τ_2, i.e., 60°, 180°, and 300°, there are two wells in 4-space. One well is sharply defined, centered at $(\tau_3, \tau_4) = (60°, 180°)$; the other much larger and more variable extending over much of the range $150° < \tau_3 < 330°$ and $30° < \tau_4 < 330°$ (see Figure 2c, for instance). Typically these two wells are separated by barriers of more than 8 kcal/mol, though at two places $(\tau_1, \tau_2, \tau_3, \tau_4) = (280°, 300°, 120°, 180°)$ and $(240°, 60°, 0°, 180°)$, the barrier is near 7 kcal/mol (see Figures 4 and 5, respectively). Within the larger of these wells there are three prominent preferred conformations: $(\tau_3, \tau_4) = (300°, 180°)$, $(300°, 300°)$, and $(180°, 60°)$. These, called conformations B, A, and D, respectively, plus the $(\tau_3, \tau_4) = (60°, 180°)$ conformation, C, are marked in Figures 4 and 5.[26]

Conformational energy barriers between the global minimum and the extended form can be estimated by taking into account conformational barriers not visible in Figure 1. Whereas this map suggests that the barrier is no higher than ≈3 kcal/mol between the two folded conformations, it is in fact not possible to go from the global minimum ($\tau_2 = 70°$) to the lowest point found in the low-energy region near $\tau_2 = 300°$ without a τ_3–τ_4 conformational change that involves crossing a barrier of 6.5 kcal/mol between the two major wells in τ_3–τ_4 space. That is, a 6.5 kcal/mol barrier is hidden there within the 2 kcal/mol area of the minimized τ_1–τ_2 map (Figure 1). This barrier can be seen at $(\tau_3, \tau_4) = (120°, 180°)$ in the τ_3–τ_4 map (Figure 4), and it can also be traced from

(24) Figure 1 is a projection from τ_1–τ_2–τ_3–τ_4 space into the τ_1–τ_2 plane. τ_3 and τ_4 generate the orthogonal complement.

(25) That is, Figure 2a is not a projection but a (three-dimensional) section.

(26) Figure 4 is the section at $\tau_2 = 300°$ in Figure 2a where the favored conformations are also apparent. It is also the section at $\tau_1 = 280°$, $\tau_2 = 300°$ in the four-dimensional cube described above. Similarly, Figure 5 is the section at $\tau_1 = 240°$, $\tau_2 = 60°$.

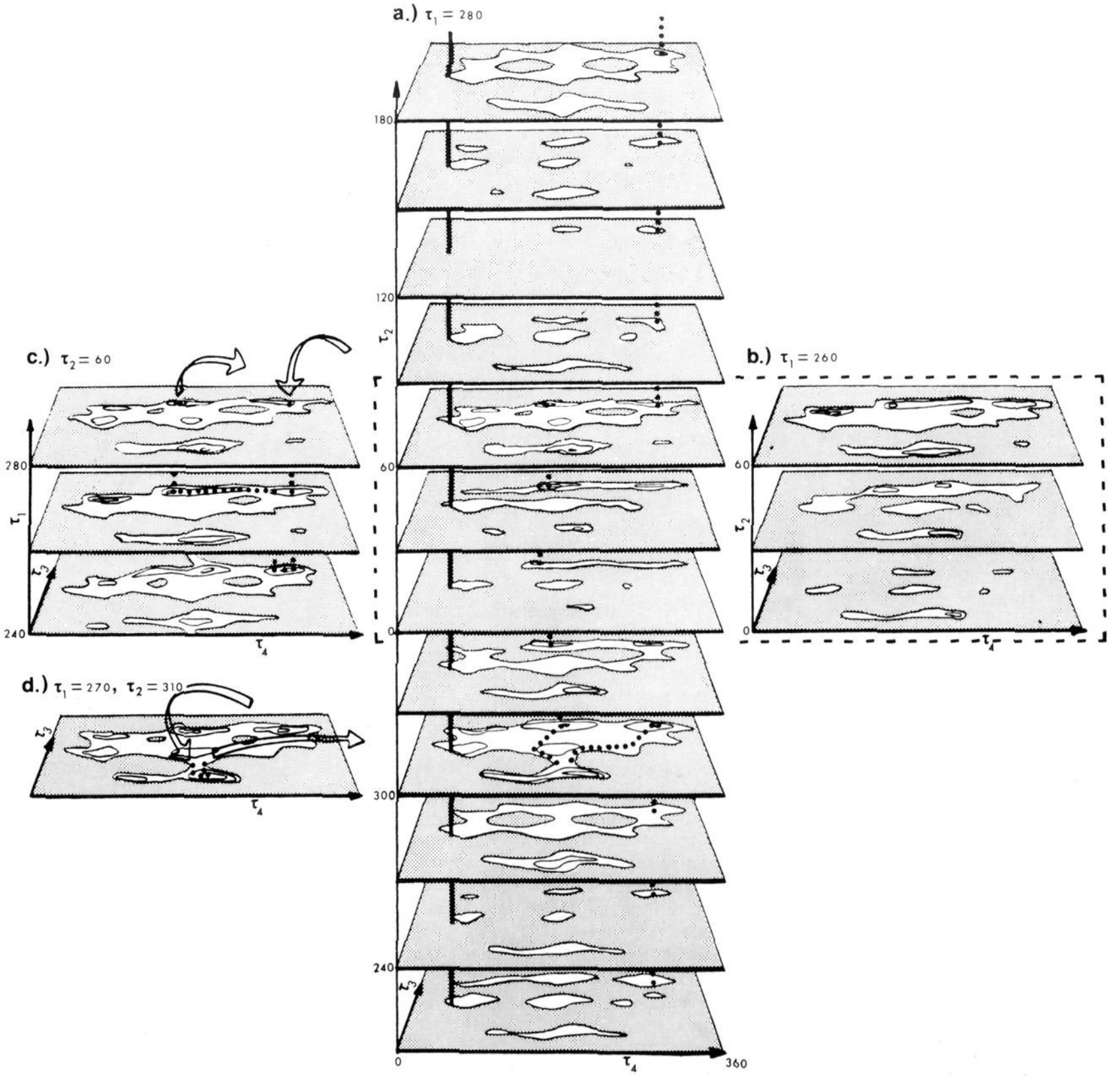

Figure 2. Sections from 4-space. Path marked (···) joins three major low energy regions. (a and b) Sections at $\tau_1 = 280°$ and $\tau_1 = 260°$, each forming a cube in τ_2, τ_3, τ_4 space. Together these views include the four-dimensional cube $260° \leq \tau_1 \leq 280°$ and $0° \leq \tau_2 \leq 60°$ in 4-space. (c) Section at $\tau_2 = 60°$, forming a cube in τ_1–τ_3–τ_4 space. Arrows indicate continuation of path ··· from (a) and (c) and back to (a). (d) Section at $\tau_1 = 270°$, $\tau_2 = 310°$. Arrows indicate continuation of path marked (···). Contours at 2 and 4 kcal/mol above the global minimum. Shaded areas >8 kcal/mol. Heavy vertical line cutting left sides of planes in (a) added to emphasis perspective.

section to section in Figure 2. The lowest energy pass found across it is indicated with the symbol] [in Figure 1 near $\tau_2 = 300°$.[27] The next lowest energy crossing between these two wells occurs near the global minimum. It is apparent in Figure 5. It too is indicated with the symbol] [in Figure 1.

Figures 6 and 7 are sketches of energy variation along two paths selected in 4-space joining the local minima. For each of the paths the (τ_1, τ_2) values are shown in Figure 1. Arc length in Figure 1 is taken as the horizontal parameter in Figures 6 and 7, and the axis is darkened where points of the path have $\tau_1 = 280°$. The chain conformations that approximately determine the (τ_3, τ_4) values are written on the graphs. The two sketches are drawn to highlight the interdependence of energy variation with conformational change in *all four* variables.

Thus, most of the paths marked (···) in Figure 1, along which the energy varies as shown in Figure 6, is the projection in τ_1–τ_2 space of the path similarly marked in the three-space $\tau_1 = 280°$ (Figure 2a) and also in Figure 2c where the crossing of the barrier between conformations A and B is shown. Part of the path also appears in the τ_3–τ_4 plane in Figure 4, where the >6 kcal/mol barrier between conformation C and conformations A and B is clearly distinguishable.

The sketch in Figure 7 for the path marked (- - -) in Figure 1 shows energy variation along an alternative low-energy route. The crossing of the region $90° \leq \tau_2 \leq 270°$ is done in conformation A, and the crossover between the folded minima is done in conformation C (see Figure 2b). Part of the path corresponding to crossing a barrier between conformations A and C is shown in Figure 5; another coincides with a portion of the path (···) in Figure 4.

Figure 1 clearly suggests the "double pass" across the central ridge near $\tau_2 = 0°$ at $\tau_1 = 260°$ in conformation C and at $\tau_1 =$

(27) It may be noted that this pass between conformations B and C is near the local minimum in this region of τ_1–τ_2 space, well within the area in which the predominent τ_3–τ_4 form is conformation C. The energies of B and C are very close here, and the lowest energy crossover between the two occurs where each is at its lowest energy, viz., near the local minimum. It should not be assumed that a low-energy pass between two preferred τ_3–τ_4 conformations should be found at junctons of areas of preferred τ_3–τ_4 conformations shown on the minimized τ_1–τ_2 map.

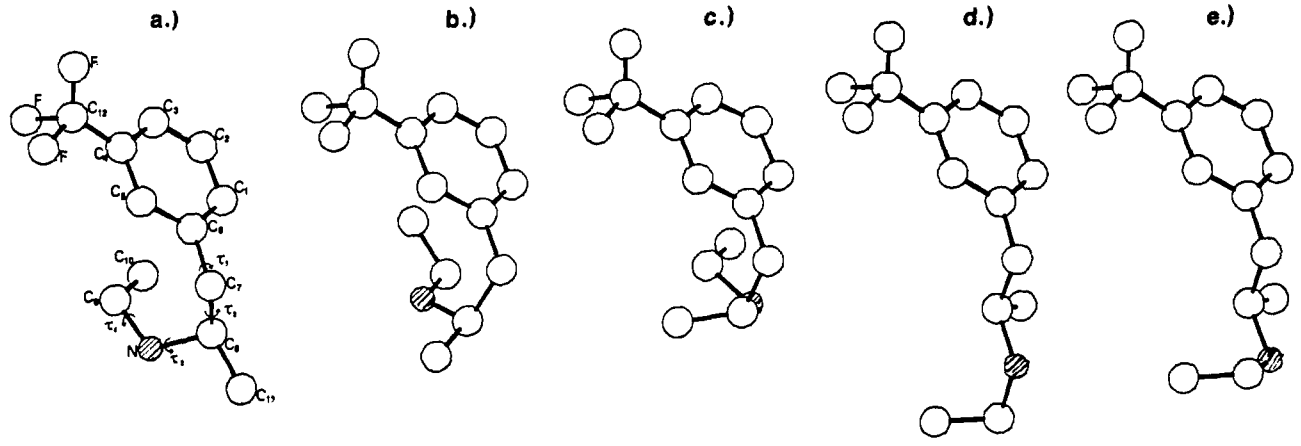

Figure 3. ORTEP drawings illustrating preferred conformations for folded and extended forms of fenfluramine and also a perferred conformation at the central ridge. Directions of rotation for torsion angles are indicated with the arrows on (a). (a) Global minimum conformation: $\tau_1 = 240°$, $\tau_2 = 70°$, $\tau_3 = 300°$, $\tau_4 = 300°$. Conformation A in τ_3–τ_4, with C_8, N, C_9, and C_{10} lying in a partial ring conformation folded under the aromatic ring. The C_9–C_{10} bond is parallel to C_6–C_1. (b) Central ridge conformation: $\tau_1 = 280°$, $\tau_2 = 0°$, $\tau_3 = 290°$, $\tau_4 = 140°$. Conformation B in τ_3–τ_4, with C_{12}, C_8, N, C_9, and C_{10} lying approximately in a staggered chain conformation, folded under the aromatic ring. (c) $\tau_2 = 310°$ local folded minimum conformation: $\tau_1 = 270°$, $\tau_2 = 310°$, $\tau_3 = 80°$, $\tau_4 = 200°$. Conformation C in τ_3–τ_4. C_8, N, C_9, and C_{10} lie in a staggered chain folded under the aromatic ring. (d and e) $\tau_1 = 260°$, $\tau_2 = 180°$, $\tau_3 = 180°$, $\tau_4 = 60°$ and $\tau_1 = 260°$, $\tau_2 = 180°$, $\tau_3 = 300°$, $\tau_4 = 300°$, respectively, typifing extended conformations. (d) illustrates conformation D in τ_3–τ_4, and C_8, N, C_9, and C_{10} lie in a partial ring. The τ_3–τ_4 angles in (c) lie in the A partial ring conformation.

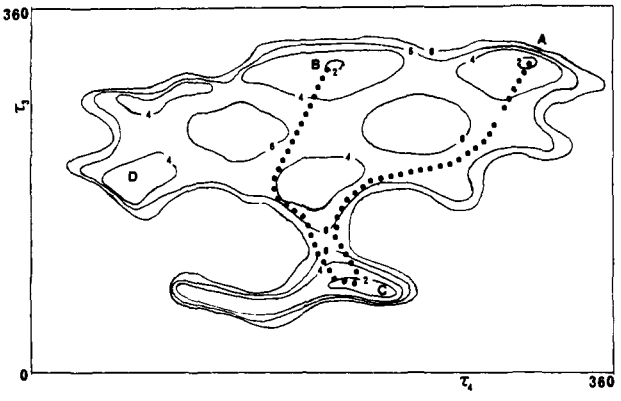

Figure 4. The section at $\tau_2 = 300°$ from Figure 2a. Preferred conformations are marked A, B, C, and D. The barrier between conformation C and the other three is obvious at $(\tau_3, \tau_4) = (120°, 180°)$.

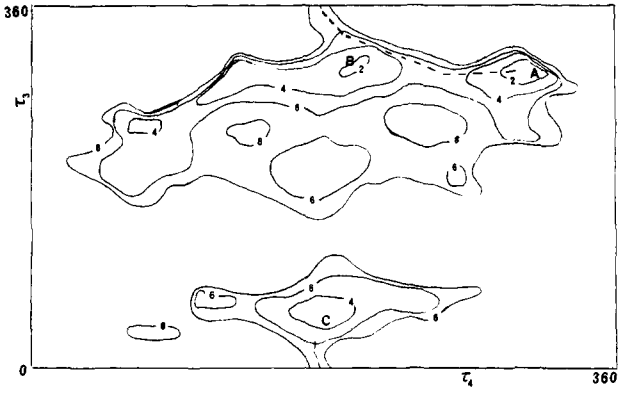

Figure 5. The τ_3–τ_4 section for $\tau_1 = 240°$, $\tau_2 = 60°$ showing alternative crossing, $(\tau_3, \tau_4) = (0°, 180°)$, between conformation C and conformations A and B (compare Figure 4). (This section shows the 2 kcal/mol region at conformation A: for these particular τ_1–τ_2 values the C conformation region is >2 kcal/mol.)

280° in conformation B. Other τ_3–τ_4 conformation changes required in going from folded to extended conformations (either from the region of the $\tau_2 = 70°$ folded minimum to the extended form or from the region of the $\tau_2 = 310°$ folded minimum to the extended form) involve energies that are essentially the same as the barriers found in the τ_1–τ_2 plane. Therefore, crossing these barriers does not require further energy input.

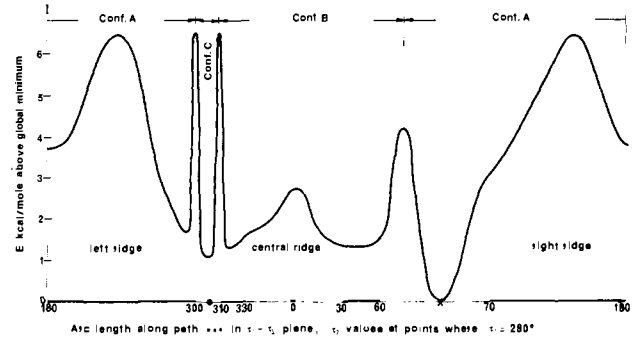

Figure 6. Minimized energy profile along path in 4-space marked (···) in Figures 1 and 2.

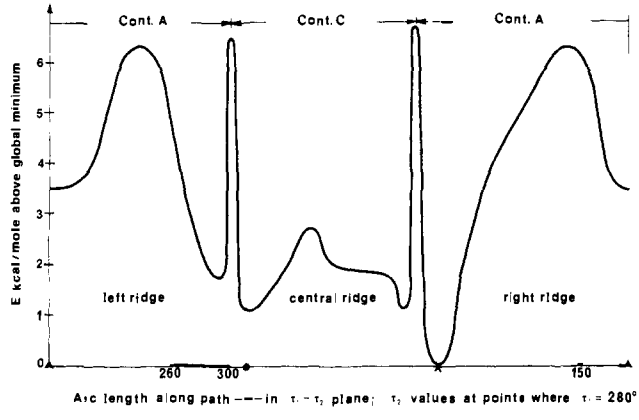

Figure 7. Minimized energy profile along path in 4-space marked (---) in Figure 1.

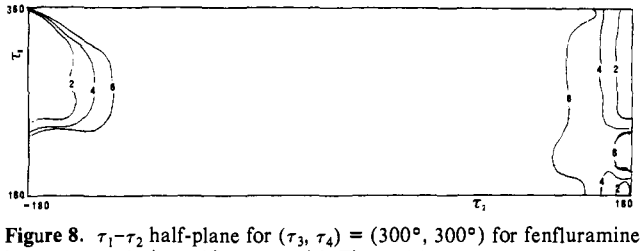

Figure 8. τ_1–τ_2 half-plane for $(\tau_3, \tau_4) = (300°, 300°)$ for fenfluramine in aqueous solution. (Contrast with Figure 1.)

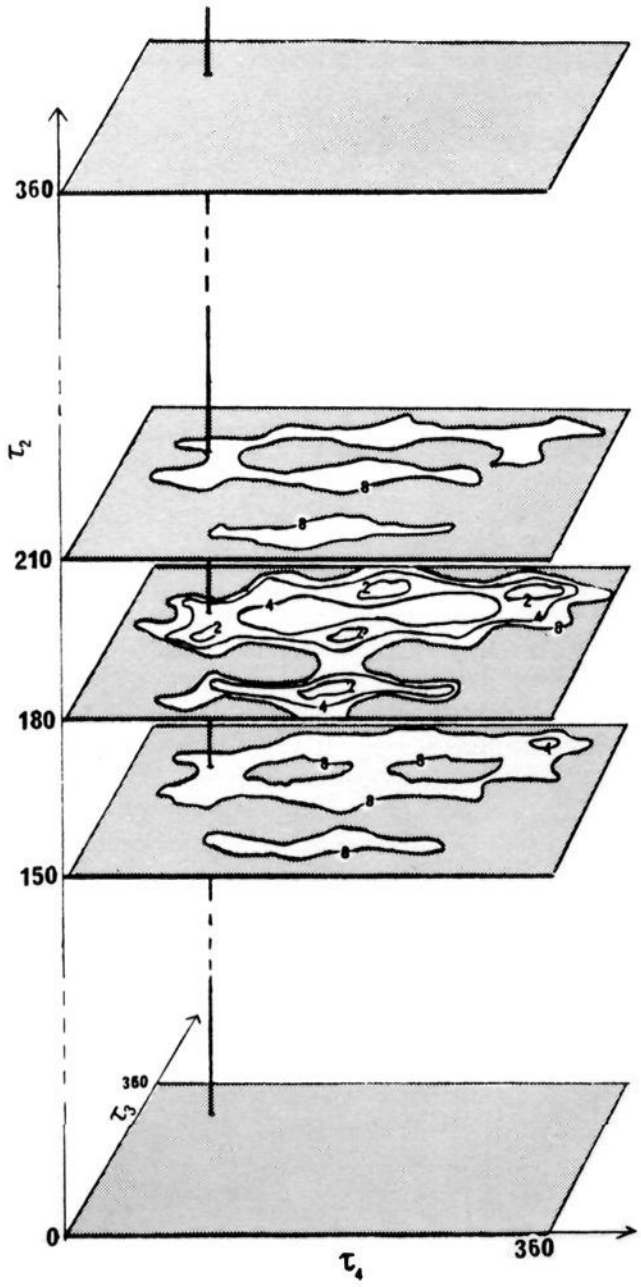

Figure 9. τ_2, τ_3, τ_4 diagram (τ_1 = 280°) for energy surfaces of fenfluramine in aqueous solution, illustrating reduction of the region of conformational stability (energies <8 kcal/mol) to three planes centered around τ_2 = 180°. (Contrast with Figure 2a.) Contours at 2 and 4 kcal/mol above the global minimum. Shaded areas >8 kcal/mol.

It may be noted that the region of the τ_2 = 310° low-energy area was subjected to a 10° increment search in 4-space in the determination of its minimum energy value. A finer search might possibly reveal some other minimum, which could, therefore, change the relative depths of the local minima in Figures 6 and 7. However, in this region, the two preferred conformations (B and C) at approximately 1 kcal/mol above the global minimum, whichever conformation may be lower, are separated by a barrier of approximately 6.5 kcal/mol.

Energies in Solution. Figure 8 shows conformational energies in aqueous solution[28] as a function of τ_1, and τ_2 (the half-plane 180° < τ_1 < 360°) for $\tau_3 = \tau_4$ = 300°. Since τ_1–τ_2 solution maps are very similar for all the prominent τ_3–τ_4 conformations, minimization was not considered worthwhile. The minimum-energy τ_2 conformation, and the only low-energy form in solution, is the extended form (τ_2 = 180°). The solution global minimum is 26.8 kcal/mol below that in vacuum. The three-dimensional diagram simplifies in solution to three significant planes centered around τ_2 = 180° (Figure 9). At this value τ_3 and τ_4 may assume any conformation; i.e., all the prominent τ_3–τ_4 conformations give low

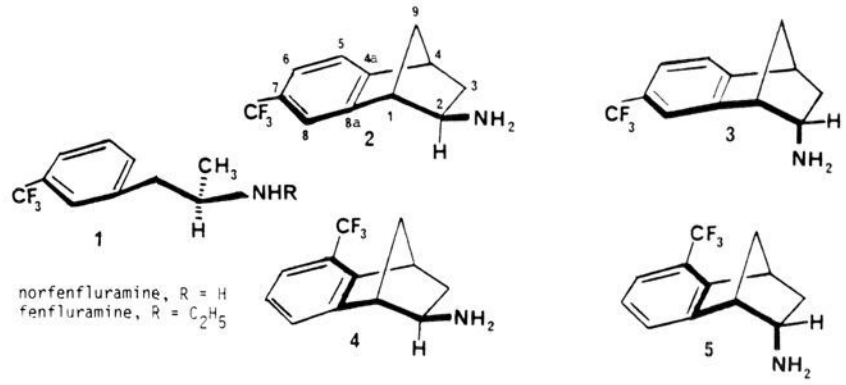

Figure 10. Conformationally defined analogues of norfenfluramine.

energies for this value of τ_2. A change of 30° in τ_2 in either direction from 180° leads to considerable energy increase and puts the system out of the stable extended conformation region.

Summary of Graphical Procedures. Since there is no simple way of diagraming in more than three variables on a two-dimensional page, it is necessary here to present the picture either as pieces or as distortions. Generally speaking, details are offered in supplementary views.

Figures 2d, 4, and 5 show two-dimensional sections. Energy variation on sections is continuous, and the contours show energies at points of space that are completely specified by the positions in the sections.

Figure 2 shows three-dimensional sections viewed straight on. These are represented as stacks of two-dimensional sections, on which contours show the intersection with surfaces of constant energy. Prespective is used to give a three-dimensional effect. (Figure 9 illustrates an oblique view of a geometrically similar section. Because of their simplicity and regularity, Figures 8 and 9 together give a good impression of the four-dimensional space for energies in solvent.)

Figure 2a, shows a small four-dimensional cube. More two-dimensional sections would have shown more detail or more space but at the cost of making the figure harder to read.

By comparison with Figure 2, Figure 1 is easy to read but somewhat misleading because the τ_3–τ_4 conformation corresponding to the energy varies from point to point. The τ_3–τ_4 maps reveal the importance of the barriers which Figure 1 does not show.

Figures 6 and 7 are actually two-dimensional sections through the energy surface in τ_1–τ_2–τ_3–τ_4–E space (five dimensional), pieced together as cut along more or less straight line segments along a path in τ_1–τ_2–τ_3–τ_4 space. In such a view the energy variation is brought out with most emphasis, at the cost of being less explicit about the location of the path.

Comments on Pharmacology. The barrier between the folded and extended forms of fenfluramine appears from these calculations[30] to be about double that in amphetamine. This suggests that the differences in pharmacology between these two drugs are due to a difference in the conformer population as they approach and bind to their receptor surfaces. One approach to the testing of this hypothesis has already been initiated:[32] it involves the synthesis of conformationally defined analogues of amphetamine and fenfluramine. We have shown dramatic pharmacological differences between ampehtamine and conformationally defined analogues of amphetamine in which either a fully extended or a gauche conformation is maintained (e.g., *exo*- vs. *endo*-2-aminobenzonorbornene).[33,34] Preliminary studies on conforma-

(28) The model used in the solution energy calculations is that developed for ionic species such as the cationic ammonium group and tested for protonated phenethylamine model compounds. See ref 29. Although the model used to compute the solvation energies has limitations, making the solvated conformational behavior results qualitative rather than quantitative, the results are in good agreement with NMR studies (unpublished results with Professor Alex Makryannis, University of Connecticut) which indicate that fenfluramine in solution is present predominantly in the trans form.

(29) Weintraub, H. J. R.; Nichols, D. E. *Int. J. Quantum Chem., Quantum Biol. Symp.* **1978**, *No. 5*, 321–343.

(30) The reliability and accuracy of barrier heights obtained by means of rigid geometry calculations are open to question. We have investigated both amphetamine and *N*-ethylamphetamine using the Flexible Intra- and Intermolecular Empirical Potential Function Method developed by Maggiora and coworkers.[31] We find that this method and CAMSEQ give similar values (~3.5 kcal/mol) for the barrier in amphetamine,[19] but in the *N*-ethyl system the barrier obtained by CAMSEQ is almost twice that found by the flexible geometry method (~3.5 vs. 6.5 kcal/mol). Previous calculations[20] by the CNDO/2 method also give an energy barrier between the folded and extended forms of *N*-ethylamphetamine of ~8 kcal/mol.

(31) Oie, T.; Maggiora, G. M.; Christoffersen, R. E.; Duchamp, D. J. *Int. J. Quantum, Chem., Quantum. Biol. Symp.* **1981**, *No. 8*, 1–47.

(32) Rafferty, M. F.; Grunewald, G. L. *Mol. Pharmacol.* **1982**, *22*, 127–132.

tionally defined analogues of norfenfluramine (also in the benzonorbornene system) have shown dramatic differences in pharmacology between the trans-anti-periplanar (Figure 10, structures **2** and **4**) and the gauche (structures **3** and **5**) conformations.[32] Furthermore, a dramatic difference between the two meta rotamers (5- vs. 7-(trifluoromethyl)-2-aminobenzonorbornene, Figure 10, **2** vs. **4**) was noted. Both the 5- and 7-trifluoromethyl rotamers approximate the global minimum found in these calculations; $\tau_1 = 270°$ and 90°. That the rigid analogues of these two equivalent minimum energy conformations show different pharmacological effects suggests a steric or electrostatic role for the CF_3 group rather than a conformational effect about τ_1.

Acknowledgment. This work was supported by U.S. Public Health Service Research Grants DA 01990 and GM 22988. We thank Dr. H. J. R. Weintraub (Eli Lilly Research Laboratories) for providing us with the CAMSEQ program and for assistance in making it operational on the University of Kansas Honeywell 66/60 system; the skillful assistance of James Wiley in the latter endeavor is also gratefully acknowledged. Figure 2a was produced photographically by Charles Andrew (Graphic Arts, Center for Research, Inc., University of Kansas). Figures 2b–d and 9 were drawn by Professor Thomas Creese (Department of Mathematics, University of Kansas), who also provided extensive assistance in the handling and interpretation of the four-variable data.

Registry No. Fenfluramine, 458-24-2.

(33) Grunewald, G. L.; Reitz, T. J.; Hallett, A.; Rutledge, C. O.; Vollmer, S.; Archuleta, J. M., III; Ruth, J. A. *J. Med. Chem.* **1980**, *23*, 614–620.
(34) Grunewald, G. L.; Borchardt, R. T.; Rafferty, M. F.; Krass, P. *Mol. Pharmacol.* **1981**, *20*, 377–381.

High-Resolution ^{13}C CP/MAS NMR Spectra of Solid Cellulose Oligomers and the Structure of Cellulose II

R. L. Dudley,[†] C. A. Fyfe,*[†] P. J. Stephenson,[†] Y. Deslandes,[‡] G. K. Hamer,[‡] and R. H. Marchessault*[‡]

Contribution from The Guelph Walterloo Centre for Graduate Work in Chemistry, Department of Chemistry, University of Guelph, Guelph, Ontario N1G 2W1, Canada, and Xerox Research Centre of Canada, Mississauga, Ontario L5L 1J9, Canada. *Received September 28, 1982*

Abstract: High-resolution solid-state ^{13}C NMR spectra of cellulose II samples and of the complete series of solid cellulose oligomers up to cellohexaose have been obtained by using cross-polarization/magic-angle spinning (CP/MAS) techniques. Comparison of the spectra of the solid oligomers with those of cellulose II preparations indicates that the characteristic features of the cellulose II structure appear in the cellotetraose spectrum and are fully developed in those of cellopentaose and of the higher oligomers. Thus a single-crystal X-ray structure determination on one of the higher oligomers should reveal the details of the cellulose II structure that the ^{13}C NMR data suggest is made up of two independent chains. A comparison of the chemical shifts for samples of cellulose I, II, and IV shows characteristic displacements of C-4 and C-6 carbons for each polymorph.

Cellulose, a major constituent of plant cell walls, is the β-1,4-polymer of anhydroglucose (**1**). In the solid state it exists

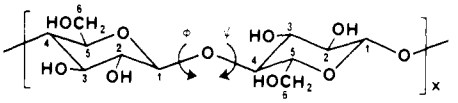

1

in at least four distinct polymorphic forms, the most common of which are named cellulose I and cellulose II.[1] Cellulose I is the natural (native) polymorph and invariably occurs with a high degree of crystallinity; depending on the source,[2] the crystallinity can range from 60% to 90%. The cellulose II polymorph is obtained by mercerization or regeneration of cellulose from solution. If regeneration is carried out at high temperatures, cellulose IV can be produced. All regenerated celluloses have a much lower degree of crystallinity (e.g., ~40%) than the native form.

Several attempts at elucidating the three-dimensional structures of cellulose I and II have been made by using modern fiber diffraction methodology and sophisticated computer modeling.[3] The important conclusion of these studies was that native cellulose with its microfibrillar texture had a parallel chain polarity, while the chain arrangement in cellulose II was antiparallel. Since the needle-like microfibrils of cellulose I are thought to be nascent (i.e., the product of a simultaneous polymerization and crystallization), the occurrence of a polymorph with antiparallel chain polarity confirms that native cellulose is a metastable form that is the consequence of a biosynthetic imperative. Biopolymer specialists would welcome a physical technique that would provide evidence of chain polarity in the crystal. High-resolution ^{13}C cross-polarization/magic-angle spinning (CP/MAS) NMR promises to be such a technique since crystal symmetry can lead to multiple signals from carbon atoms that are chemically identical but crystallographically inequivalent.

The techniques of cross-polarization and magic-angle spinning have been developed in recent years to yield high-resolution NMR spectra of dilute nuclei (e.g., ^{13}C) in the solid state.[4] The chemical shift values of these spectra are the isotropic values (for the solid state), which are similar to those obtained in solution and may be used for structural elucidation in terms of both molecular and crystal structures. In the particular case of cellulose, spectra have

[†] University of Guelph.
[‡] Xerox Research Centre of Canada.
(1) Bikales, N. S.; Segal, L. "Cellulose and Cellulose Derivatives—Part V, High Polymers" 2nd edn.; Wiley-Interscience: London, 1971.
(2) Warwicker, J.; Jeffries, R. *Shirley Inst. Pam.* **1966**, *No. 93*.
(3) (a) Gardner, K. H.; Blackwell, J. *Biopolymers* **1974**, *13*, 1975–2001. (b) Sarko, A.; Muggli, R. *Macromolecules* **1974**, *7*, 486–494.
(4) (a) *Philos. Trans. R. Soc. London, Ser. A* **1981**, *299*, 1452. (b) Lyerla, J. R. *Contemp. Top. Polym. Sci.* **1979**, *3*, 143–213. (c) Fleming, W. W.; Fyfe, C. A.; Kendrick, R. D.; Lyerla, J. R.; Vannie, H.; Yannoni, C. S. *ACS Symp. Ser.* **1980**, *No. 142*, 193–217. (d) Yannoni, C. S. *Acc. Chem. Res.*, in press. (e) Fyfe, C. A.; Lyerla, J. R.; Yannoni, C. S. *Ibid.*, in press. (f) Wasylishen, R. E.; Fyfe, C. A. *Annu. Rep. NMR Spectrosc.*, in press.

0002-7863/83/1505-2469$01.50/0